Hongxin Wang, Nadezda Slavinskaya, Aziza Kanz, Moldir Auyelkhankyzy, Yiting Gao, Oskar Haidn

A Comprehensive Kinetic Modeling Study of Ethylene Combustion with Data Uncertainty Analysis

Fuel

Volume 299, 1 September 2021, 120833

The original publication is available at www.elsevier.com

https://doi.org/10.1016/j.fuel.2021.120833

A Comprehensive Kinetic Modeling Study of Ethylene Combustion with Data Uncertainty Analysis

Hongxin Wang[a], Nadezda Slavinskaya[b, c], Aziza Kanz[d], Moldir Auyelkhankyzy[c, e], Yiting Gao[a], Oskar Haidn[a]

a. Department of Aerospace and Geodesy, Technical University of Munich, 85748 Garching, Germany

b. GRS Association for Plant and Reactor Safety, 85748 Garching, Germany

c. Al-Farabi Kazakh National University, 050040 Almaty, Kazakhstan

d. DLR German Aerospace Center, Institute of Combustion Technology, 70569 Stuttgart, Germany

e. Institute of Combustion Problems, 050012 Almaty, Kazakhstan

Abstract

A revision and upgrade of the ethylene (C_2H_4) oxidation kinetic sub-mechanism were carried as a next step in the optimization of the $C_{<3}$ chemistry, which is a base for the upcoming PAH sub-model improvement. The main emphasis of the work was focused on the assessment of uncertainties of the thermo-kinetical and experimental data used to achieve the reasonable model parameter corrections. The principal targets of mechanism extension and update are: inspection of the reaction rate coefficients with accounting recently published pressure-dependent reactions and analysis of reaction paths related to the C_2H_4 low-temperature oxidation and the formation of aromatic precursors. The experimental data (auto-ignition, premixed laminar flame speeds, and concentration profiles) with evaluated uncertainty and consistency were used for model optimization. The uncertainty bounds of the key reaction rate coefficients were evaluated from the statistical treatment of the published data, which provided constraints in the reaction rate parameters. The rate parameters of 57 reactions of C_2H_4 and key intermediates were optimized. The revised reaction mechanism demonstrates a good agreement with the majority of the existing experimental data. Results of the sensitivity and rate of production analyses were performed for several kinetic mechanisms from the literature and compared to visualize the variations and ambiguity in the importance of reaction paths and highlight the problems in mechanism optimization and integration.

Keywords: ethylene, chemical kinetic mechanism, uncertainty, auto-ignition, laminar flame

1. Introduction

Ethylene (C_2H_4) is an important fuel and a key intermediate in the combustion of hydrocarbons. Its oxidation and pyrolysis reactions are also important for the formation of polycyclic aromatic hydrocarbons (PAH) and soot precursors. The C_2H_4 chemistry has been explored in sufficient breadth and depth over the past decades [1-10] to assume that the completeness of current chemistry is achieved and most important qualitative improvements of models could be done by further optimizations of poorly understood reaction rate coefficients (RRC).

Despite great efforts and constantly emerging new data, most elementary reaction rate parameters are not known with sufficient accuracy [11-14], moreover, uncertainties of the available data remain unknown in most cases. By that, the reaction mechanism updating can become a permanent process, which initiates the question: what is the final version and how can we define that? The easiest answer is making sure that all the conceivable reactions are included and all RRCs in the model are obtained from the "first principals" with acceptable accuracy. However, it is not yet possible now. We do not have a hallmark to be sure a model includes all conceivable reactions. The RRCs from "first principals" are restricted, in the case of experiments, by ranges of measurement conditions and parameter fitting, and in the case of quanta-chemical calculations, by applied theoretical evaluations and numerical methods.

Therefore, most of the RRCs, especially for $C_{\geq 2}$ fuels, are derived from semi-empirical methods and model calibrating against combustion data performed by different workgroups. Some of these RRCs are successfully used in different reaction mechanisms, which will be regarded as statistical samplings, so these RRCs can be classified as "quasi first principal" empirical data of high quality. Unfortunately, significantly more data obtained in this way were evaluated for conditions of the individual study interest or from fitting the model parameters to better match some experimental data within their respective range of applications. The development of numerical tools for reaction model fitting can further sharpen this problem: direct matching the experimental data of the different quality

levels can lead to unwarranted modifications of the RRCs, which can be further traced in different models published in the literature. In the following analysis of model parameters, we tried to recognize these problems.

Detailed reaction mechanisms of hydrocarbon combustion chemistry have the hierarchical structure and logical passes from H_2 to larger chemical species with offshoots for pollution formation (NO_x, sulfuric acid, PAH, soot, etc.). It remains unclear [15] whether RRCs derived by optimization of small hydrocarbon mechanisms need to be re-optimized by modeling the oxidation of larger fuel molecules. We assumed that the re-optimization of some empirical RRCs by the optimization and extension in the next hierarchy sub-model is inevitable. Such re-optimization was performed through calibration of all "smaller" sub-models and was adopted only if the facility of sub-models were not disturbed. Parameters of RRCs obtained from the first principal were re-optimized exclusively if the new data of higher quality were published or found. We keep this strategy to reduce re-optimization efforts and to narrow the uncertainty intervals of the "anchoring reactions" which support the structure of the reaction database under development.

The work presented in this study belongs to the upgrade of the kerosene combustion model with PAH formation [9, 10, 16-19]. Now the C_1-C_3 oxidation chemistry is under optimization without changes in the PAH formation sub-mechanism. This chemistry will be updated after the final inspection of the C_1-C_3 oxidation chemistry. The reaction paths for the PAH formation are strongly coupled with both $C_{\leqslant 3}$ chemistry and the products of the larger hydrocarbons, part of which are the PAH precursors. The including PAH reactions in the C_1-C_3 oxidation chemistry allow avoiding the model tailoring and the artificial breaking of the atom flows, and serve as a bridge between small and large molecules oxidation. The well-parameterized detailed chemistry of PAH precursors is expected to reduce the re-optimization efforts in upcoming updates of the $C_{\geq 4}$ combustion chemistry models.

Another reason for following this strategy is the extremely high data scattering for kinetics of poly-aromatic molecules. Despite high-level theoretical calculations, the progress here can be achieved

through the model calibration against measured concentration profiles, which follow mostly from the small-molecule combustion study. The well-optimized small chemistry can increase the chance to obtain stable and physically reasonable parameters of RRCs for PAH reactions in the future.

In this paper, we report the C_2H_4 sub-mechanism optimization which continues the preparation of the basic small chemistry reaction model [17, 18, 20, 21]. The optimization is based on the first principals considering the most recent investigations and discoveries in the field of kinetic chemistry with estimated uncertainties and the comprehensive model validation against representative high-fidelity experiments for a wide application domain. All the calculations were performed with the Ansys Chemkin Pro [22] software. The model inspection and optimization were based on the following axes: (1) final issue of the reaction mechanism for acetylene combustion [17]; (2) the literature review and analysis of the components and reactions involved in the ethylene oxidation; (3) the uncertainty analysis of RRCs; (4) analysis of uncertainties and consistency of the experimental data used for model validation and optimization; (5) the model calibration and optimization on experimental data for ignition delay times, laminar flame speeds and species concentration profiles.

Considering that the studied model is a part of the reaction mechanism for kerosene combustion with PAH formation, the model is constructed to keep reasonable size, and therefore unimportant channels and channels with high level of uncertainties were ignored.

The paper is organized as follows: the second section discusses the uncertainty analysis with the statistical method and uncertainty intervals for the initial steps of C_2H_4 oxidation. The third section presents the improvements in model optimization. The fourth section reports the validation results, i.e. simulations of experimental data for ignition delay times, laminar flame speeds and concentration profiles, and discussion. Additionally, the obtained model was compared with the models for small hydrocarbons published within the last two decades, including mechanisms of Aramco 3.0 [12], USC 2.0 [11], UCSD [13], Lopez et al. [6], Konnov [14], Dias et al. [7], NTUA [2], and GRI 3.0 [23]. The

present work is supported by the supplement materials 1, 2, 3, 4, and the updated chemical kinetic model. An overview of the modeling studies listed above is presented in Supplementary-1.

2. Uncertainty bounds of the reaction rate parameters

To fix the size of the feasible parameter region and to understand the uncertainty intervals for RRCs, we performed the statistical analysis [17, 24-26] of the literature data for important reactions. The detailed theory has been presented in our former work [17], therefore only a brief review of the analysis parameters is shown here.

The standard deviations of the Arrhenius expression parameters *A*, *n*, and E_a:

$$k(T) = AT^n \exp\left(-\frac{E_a}{T}\right), (\mathrm{cm}^3, \mathrm{s}, \mathrm{mole}, \mathrm{K}) \quad (1)$$

calculated in the applied method of nonlinear regression [17, 24-26], determine the margin, $\Delta k(T)$, of the rate-coefficient error. The uncertainty factor $f(T)$ [27, 28] is used to determine the uncertainty level for $k(T)$:

$$f(T) = \log_{10}\left(\frac{k_{\mathrm{up}}(T)}{k_0(T)}\right) = \log_{10}\left(\frac{k_0(T)}{k_{\mathrm{low}}(T)}\right) \quad (2)$$

where k_0 is the nominal RRC and k_{low} and k_{up} are the lower and upper bounds respectively. Errors of the Arrhenius expression parameters [17], $s(x_a)$, describing the confidence level of RRC parameters, were used for calculation of:

$$k_{\mathrm{low}}(T) = (A - s(A))T^{(n-s(n))}\exp(-\frac{E_a+s(E_a)}{T}) \quad (3)$$

$$k_{\mathrm{up}}(T) = (A + s(A))T^{(n+s(n))}\exp(-\frac{E_a-s(E_a)}{T}) \quad (4)$$

and finally, for the evaluation of the uncertainty factors, Equation (2).

For the investigated uncertainty intervals, experimental measurements and theoretical calculations of RRCs were collected from the NIST Chemical Kinetics Database [29] and recently published references. Baulch et al. [27, 30-34] conducted a series of reviews on RRCs, but the recommendations in their early works [30-34] show relatively high uncertainties due to the limitation of available data so that only the newest work [27] was applied in the uncertainty analysis.

Table 1. Uncertainty factors calculated from the literature sources for the reaction C_2H_4 + O = products, $k(T) = AT^n exp(-E_a/T)$.

Reaction	Reference	T range, K	k, cm^3, s, mole, K		
			A	n	E_a, K
C_2H_4+OH=C_2H_3+H_2O	Ali2011 [35]	200-400	6.20E+11	0.00	1400.0
f = 0.301 – 0.318	Senosiain2006 [36]	250-2500	1.31E-01	4.20	-433.0
	Baulch2005 [27]	650-1500	2.05E+13	0.00	2990.0
	Liu2002 [37]	200-5000	2.10E+06	2.01	585.0
	Westbrook1989 [38]	1003-1253	2.00E+13	0.00	2990.0
	Tully1988 [39]	650-901	2.02E+13	0.00	2990.0
	Liu1987 [40]	748-1170	1.45E+13	0.00	2100.0
	Tsang1986 [34]	300-2500	1.57E+04	2.75	2100.0
	Warnatz1984 [33]	500-2000	3.00E+13	0.00	1500.0

The uncertainty ranges evaluated by the review work of Baulch et al. [27] are implemented in the applied statistical tool. As an example of performed statistical analysis, the obtained uncertainty factor for the reaction of C_2H_4 + OH = C_2H_3 + H_2O is shown in Table 1 and Figure 1. As mentioned above, the RRCs recommended in the early review works of Tsang et al. [34] and Warnatz [33] show high uncertainties so that RRCs from these works are depicted only for comparisons and were not applied in the statistical analysis. Other uncertainty factors and uncertainty bounds for the analyzed channels are presented in Table S2-1 and Figure S2-1 in Supplementary-2.

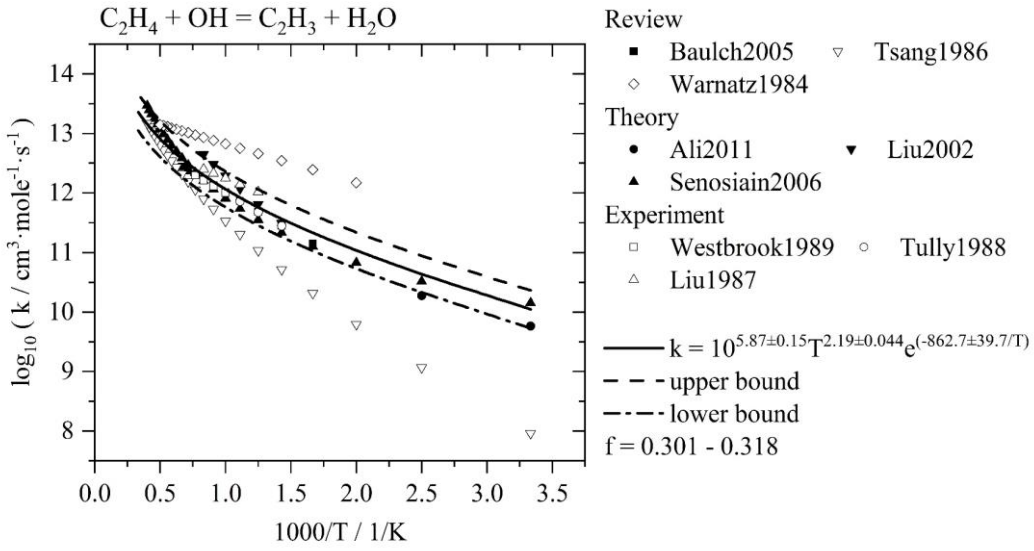

Figure 1. Determination of k_{low} (lower bound) and k_{up} (upper bound) and the uncertainty factor for the reaction C_2H_4 + OH = C_2H_3 + H_2O from the statistical analysis of the literature data (solid symbols for the data published after the year 2000, and open symbols for the data published before the year 2000).

3. Model improvements

3.1 Inspection and update of reaction rate constants

The original mechanism [17] based on our previous work [9, 10, 18, 41, 42] is referred to as model-1, and the obtained newly optimized model for C_2H_4 is referred as model-2. Our initial mechanism for the PAH formation [42] was developed on the base of methane oxidation model of Hughes et al. [41] which was constructed at that time with a tough requirement of first principal application. Over time this base principal turned into a disadvantage. For example, a number of RRCs adopted in [9, 10, 17, 18, 42] from [41] were originated from experiments relevant to the limited temperature intervals; third body reactions have a large uncertainty for low-pressure limit and collider definitions, etc. The out coming chemistry traced from the model [41] in the model releases [9, 10, 17, 18, 42] initiated the mechanism revision and improvement.

Critical analysis of matches between simulations with model-1 and experiments on ignition delay times and laminar flame speeds has been performed and highlights the problems to be solved: model-1 over-predicted ignition delay times and laminar flame speeds of C_2H_4. By scanning results of sensitivity analysis (Figure S2-2 in Supplementary-2) accounted for the representative set of experimental data, reactions with the highest potential to provide the model improvement were determined [17] and all known sources of the RRCs were analyzed. The reactions under inspection were related mostly to the low-temperature reactions of C_2H_4 oxidation and reactions of the key intermediates such as ethylenyl (C_2H_3), ethyl radical (C_2H_5), ketene (CH_2CO), and acetaldehyde (CH_2CHO). Special attention was paid to the pressure-dependent RRCs and the reactions important for the formation of PAH precursors.

The modified reactions for ignition delay times, laminar flame speeds and concentration profiles are shown in Table 2. The important reactions for different validation targets are identified through the sensitivity and rate of production analyses, the results of which will be shown in the following sections. The modifications of the RRCs are controlled within the calculated uncertainty bounds. The data

published within the last twenty years or recommendations from recently developed or updated mechanisms are preferred, but for some reactions, only a small amount of data or references could be found. The detailed description of revised reactions and modification work is reported in Supplementary-2. The collections of RRCs and the final list of updated values are shown in Table S2-1 and S2-2 in Supplementary-2.

Table 2. Reactions optimized on the measured data for ignition delay time, laminar flame speed and concentration profile.

No.	Reaction	Ignition delay time		Laminar flame speed	Concentration profile
		low-T	high-T		
R2a	$C_2H_4+O=CH_3+HCO$		√		√
R2b	$C_2H_4+O=CH_2CHO+H$		√	√	√
R2c	$C_2H_4+O=CH_2O+CH_2$			√	√
R2d	$C_2H_4+O=CH_2CO+H_2$		√		√
R3a	$C_2H_4+OH=C_2H_3+H_2O$	√	√	√	√
R3d	$C_2H_4+OH=C_2H_3OH+H$				√
R4a	$C_2H_4+H=C_2H_3+H_2$		√		√
R4b	$C_2H_4+H=C_2H_5$				√
R5a	$C_2H_4=C_2H_3+H$		√	√	√
R5b	$C_2H_4= H_2CC+H_2$	√	√		
R6	$C_2H_4+HO_2=CH_2OCH_2+OH$	√			
R7a	$C_2H_5+O_2=C_2H_4+HO_2$	√			√
R8a	$CH_3+CH_3=C_2H_5+H$			√	
R8b	$C_2H_5+H=C_2H_4+H_2$			√	
R10, R11	CH_2CO			√	√
R12	CH_3CO				√
R13, R14	CH_2CHO				√
R15-20	H_2CC		√	√	√
R21-26	CH_2OCH_2	√			

3.2 Modification of reaction rate constants

The further rate constant adjustments of the C_2H_4 chemistry rate parameters were carried out on the base of simulations of experimental data with model-2 applying sensitivity and rate of production analyses. Figure 2 illustrates the scattering in normalized sensitivity coefficients calculated for the reactions of model-2 by simulations of ignition delay times and laminar flame speeds. Top 15 reactions

related to C_2 species are shown. According to the sensitivity coefficients, channels related to O_2 and HO_2, such as reactions of $C_2H_3+O_2$, $C_2H_4+HO_2$, and $C_2H_5+O_2$, are the most important channels for the low-temperature ($T_5 \leqslant 1000$K) oxidation of C_2H_4. For the higher temperature ($T_5 = 1800$K), reactions related to O and H and the decomposition of C_2H_4 become more important, as shown in Figure 2.

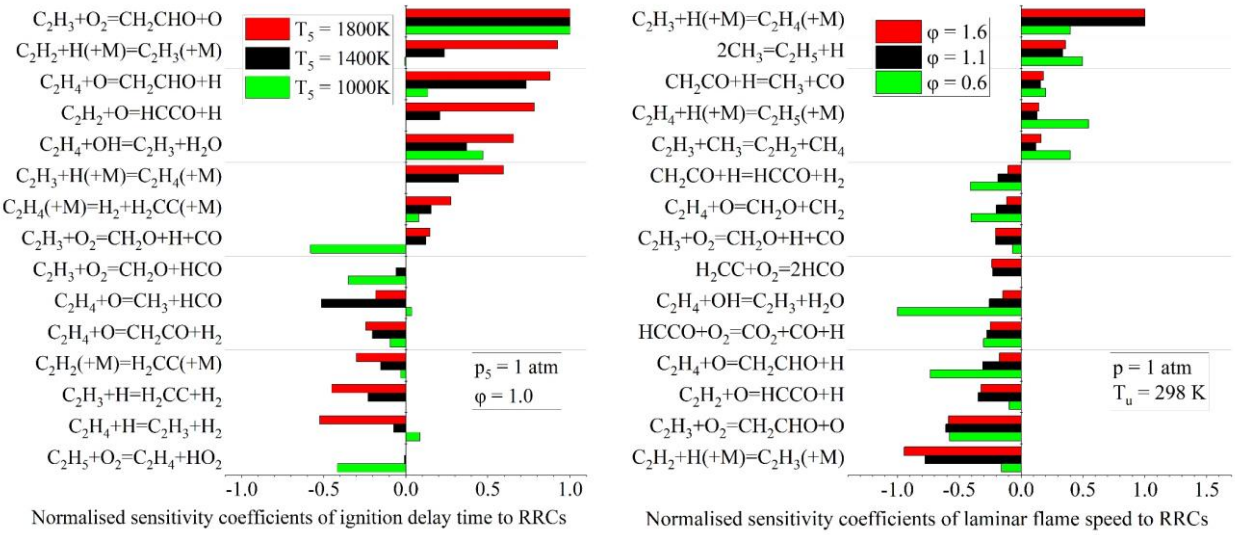

(a) **(b)**

Figure 2. Comparison of normalized sensitivity coefficients calculated with model-2 for: (a) ignition delay times of $C_2H_4/O_2/Ar$ mixtures with $\varphi = 1.0$, $p_5 = 1$ atm and $T_5 = 1000$, 1400, 1800 K; (b) laminar flame speeds of C_2H_4/air mixtures with T_u=298K, p=1 atm and $\varphi = 0.6$, 1.1, 1.6.

The optimization approach and protocol were essentially identical to the one used in [17, 21]. The *k* values to be modified were tested iteratively until the best optimization was obtained. The known kinetic data was applied in the model improvement: experimental C_2H_4 ignition delay times from publications [1, 3, 5, 43-47] measured for $T_5 = 1000$ - 2238 K, $p_5 = 1$ - 60 atm and equivalence ratios of 0.5 to 3.0; laminar flame speeds of C_2H_4/air mixtures measured by heat flux method, counter flow flames and spherical flames [48-54]; concentration profiles obtained in premixed flat flames [2, 7, 55-57], as shown in Table 3.

Table 3. Overview of the ignition delay times (ST for shock tube), laminar flame speeds (HF for heat flux method, CF for counterflow flame, SF for spherical flame) and concentration profiles (PFF for premixed flat flame) used for validation.

Ignition delay time	T_5 **/ K**	p_5 **/ atm**	**Mixture and method**
Brown et al. 1999 [43]	1074-2238	1 - 5	$C_2H_4/O_2/Ar$, φ = 1.0, ST $C_2H_4/O_2/N_2$, φ = 1.0, ST
Colket et al. 2001 [44]	1125-1380	5 - 8	$C_2H_4/O_2/Ar$, φ = 0.5 - 1.0, ST
Kalitan et al. 2005 [45]	1115-1754	1 - 3	$C_2H_4/O_2/Ar$, φ = 0.5, 1.0, ST
Penyazkov et al. 2009 [46]	1120-1520	6 - 15	C_2H_4/air, φ = 0.5 - 2.0, ST
Saxena et al. 2011 [5]	1000-1634	2 - 18	$C_2H_4/O_2/Ar$, φ = 1.0, 3.0, ST
Kopp et al. 2014 [3]	1106-1310	1 - 25	C_2H_4/air, φ = 0.3 - 1.0, ST
Deng et al. 2017 [47]	1090-1600	1.2 - 10	$C_2H_4/O_2/Ar$, φ = 1.0, ST
Shao et al. 2018 [1]	1095-1317	15, 60	$C_2H_4/O_2/Ar$, φ = 1.0, 2.0, ST
Laminar flame speed	T_u **/ K**	p **/ atm**	**Mixture and method**
Egolfopolous et al. 1991 [58]	298	1	C_2H_4/air, CF
Hassan et al. 1998 [48]	298	0.5 - 4	C_2H_4/air, SF
Hirasawa et al. 2002 [49]	298	1	C_2H_4/air, CF
Jomaas et al. 2005 [50]	298	1	C_2H_4/air, CF
Kumar et al. 2008 [51]	298	1	C_2H_4/air, CF
Park et al. 2013 [52]	298	1	C_2H_4/air, CF
Ravi et al. 2015 [53]	298	1	C_2H_4/air, SF
Treek et al. 2020 [54]	298	1	C_2H_4/air, HF
Concentration profile	T_u **/ K**	p	**Mixture and method**
Xu et al. 1997 [55]	298	98.7 kPa	C_2H_4/air, PFF
Delfau et al. 2007 [56]	298	1 atm	$C_2H_4/O_2/N_2$, PFF
Dias et al. 2011 [7]	298	0.05 bar	33%C_2H_4+40%O_2+27%Ar, PFF
Korobeinichev et al. 2011 [57]	298	0.04 bar	28%C_2H_4+42%O_2+30%Ar, PFF
Malliotakis et al. 2018 [2]	298	0.05 bar	30%C_2H_4+40%O_2+30%Ar, PFF

4. Results and discussion

4.1 Ignition delay times

The detailed experimental data and modeling results of ignition delay times are presented in Supplementary-3. Large scattering of experimental data generates difficulties for the proper optimization of the mechanism. Brown et al. [43], Kalitan et al. [45], and Saxena et al. [5] conducted shock tube experiments with the same mixture (1% C_2H_4 + 3% O_2 + 96% Ar) at similar pressure (p_5 = 1-3 atm). A comparison of these experimental data [5, 43, 45] with the modeling results simulated with model-2 is presented in Figure 3a. It can be seen that model-2 can predict the ignition delay times from

Kalitan et al. [3] and Saxena et al. [4] quite well but cannot reproduce the data measured by Brown et al. [43]. Similar results obtained by the simulation with Aramco 3.0 [12], USC 2.0 [11], and UCSD [13] mechanisms are presented in Supplementary-3, and the compared mechanisms tend to be consistent with the results measured by Kalitan et al. [3] and Saxena et al. [4].

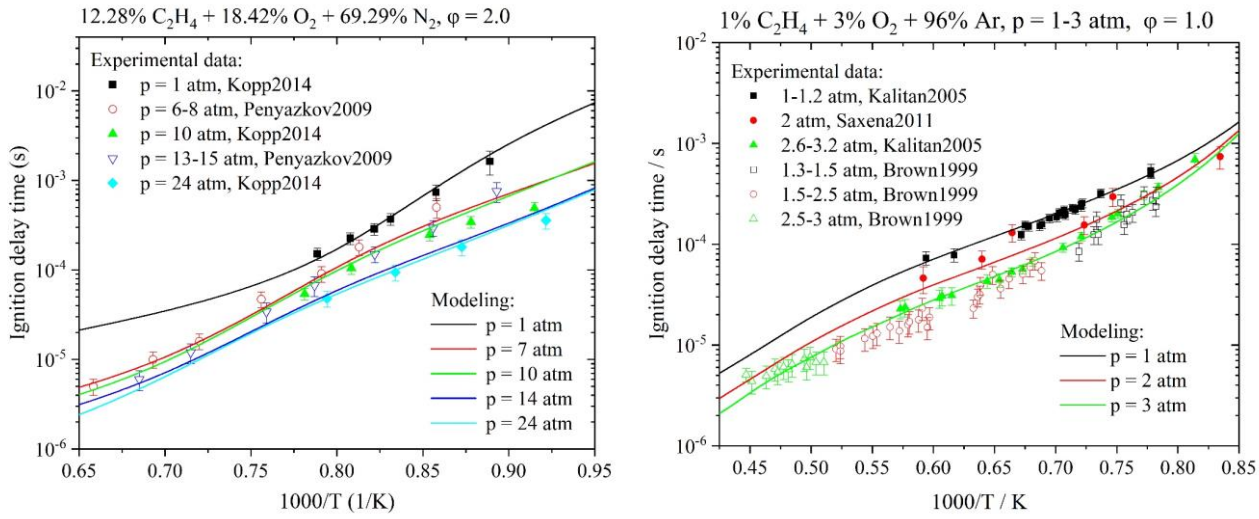

(a) **(b)**

Figure 3. The experimental ignition delay times measured by the different groups (Brown1999 [43], Kalitan2005 [45], Saxena2011 [5], Penyazkov2009 [46], Kopp2014 [3]) versus simulations performed with model-2.

The same problem occurs in the ignition delay times of the C_2H_4/air mixtures measured by Penyazkov et al. [7] and Kopp et al. [6], as shown in Figure 3b. Penyazkov et al. [7] and Kopp et al. [6] measured ignition delay times for the same mixture at different pressures with shock tubes, but the data measured by Penyazkov et al. [7] shows a trend of over-prediction at temperatures higher than 1250 K (1000/T>0.8). Figure 3 illustrates a problem arising at the model calibrating in a case of inconsistent experimental data. As the data are measured under the same conditions, the dominants reactions are the same for both measured sets. Conclusions following from these data simulations are contradictory and rate constant optimization in such cases can lead to the parameters lying beyond physical and theoretical reasonable ranges. To meet a decision about data quality, in similar controversial cases we simulated data with various models to analyze the scattering in simulations.

To follow the optimization progress, the global average error of modeling ignition delay times against the measured data is defined as follows [59]:

$$E = \frac{1}{N}\sum_{i=1}^{N}\frac{1}{N_i}\sum_{j=1}^{N_i} e_{ij} \quad (6)$$

where N is the number of data sets, N_i is the number of data points in the ith data set. The error of modeling results based on the uncertainty e_{ij} which is defined as:

$$e_{ij} = \ln\left(\frac{t_{ij}^{sim} - t_{ij}^{exp}}{u_{ij}}\right)^2 \quad (7)$$

where t_{ij}^{exp} is the experimental value of the ignition delay time, t_{ij}^{sim} is the simulated result and u_{ij} is the experimental uncertainty.

Most authors who measured ignition delay times only evaluated the uncertainties for specific experiment settings or an average uncertainty for the measured ignition delay times [1, 5, 45]. In this study, the uncertainties, u_{ij}, were evaluated based on the similar strategy shown in our previous work [21, 60]. The T_5, p_5, and equivalence ratio distribution and evaluated uncertainties of the collected 461 ignition delay time targets [1, 3, 5, 44, 45, 47] are illustrated in Figure 4a. The points are colored in green for $10\% \leq u_{ij} \leq 15\%$, blue for $20\% \leq u_{ij} \leq 25\%$, and red for $u_{ij} \geq 30\%$. The biggest uncertainties are evaluated for the data obtained mostly for fuel-rich mixtures at lower temperatures ($T_5 < 1200$K) and high temperatures ($T_5 > 1600$K), where more experimental targets are needed for uncertainty analysis and data quality analysis. Figure 4b shows the distribution of modeling errors (e_{ij}, Equation 7) for the ignition delay time targets modeling. The points are colored in green for $e_{ij} < 0.001$, blue for $0.001 \leq e_{ij} \leq 0.005$, and red for $e_{ij} > 0.005$. The biggest discrepancies have been achieved for data measured at $T_5 < 1100$K and $\varphi > 2.5$ for all studied pressures.

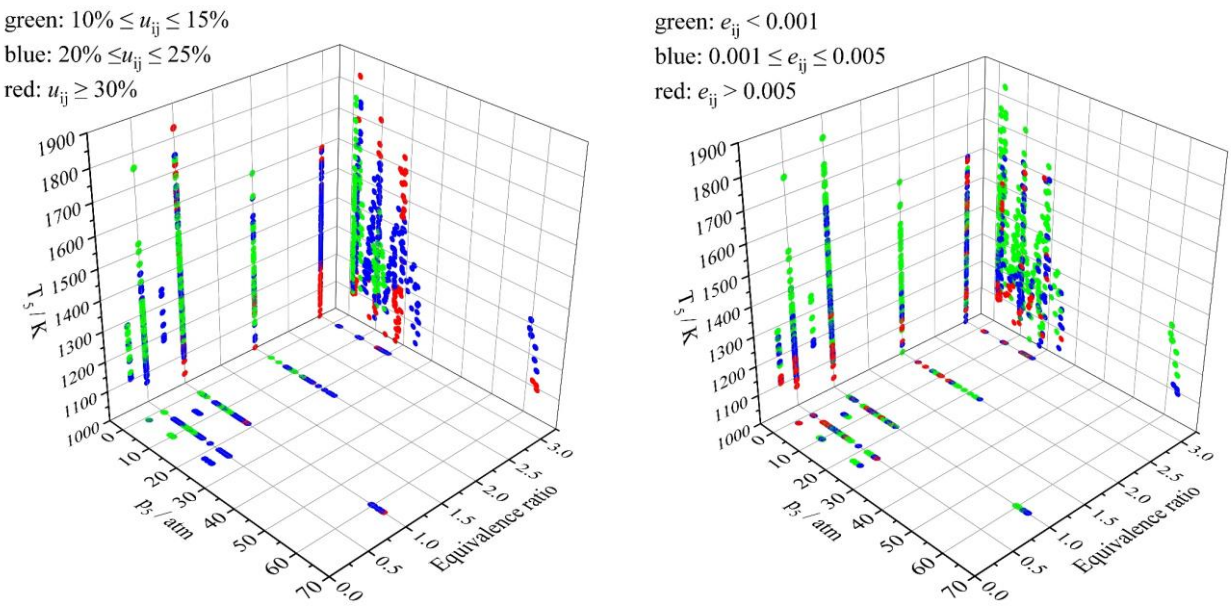

(a) **(b)**

Figure 4. (a) Uncertainties of the used experimental ignition delay times in T_5, p_5 and equivalence ratio: green points for 10% ≤ u_{ij} ≤ 15%, blue points for 20% ≤u_{ij} ≤ 25% and red points for u_{ij} ≥ 30%; (b) Errors for modeling ignition delay times with model-2: green points for e_{ij} < 0.001, blue points for 0.001 ≤ e_{ij} ≤ 0.005 and red points for e_{ij} > 0.005.

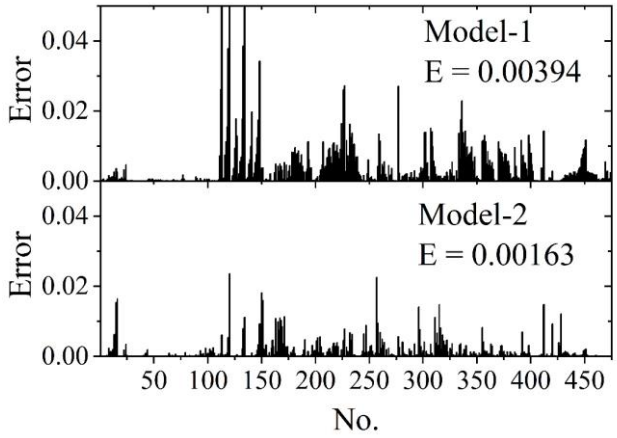

Figure 5. Modeling errors (e_{ij}, equation 7) for ignition delay times obtained with model-1 and model-2.

Figure 5 demonstrates progress in the e_{ij} (equation 7) calculated for modeling ignition delay times with model-1 and model-2. Considering the contradiction of the experimental data, the ignition delay times measured by Brown et al. [43] are excluded from the data set used for mechanism optimization. The comparison of the errors of the two models shows a significant improvement in predicting the

ignition delay times. The e_{ij} errors for other compared mechanisms [2, 6, 7, 11-14, 23] are shown in Figure S3-1 in Supplementary-3.

Although lots of ignition delay time data are measured today, it is not enough to cover all the operating conditions of practical interests. Kinetic models are generally validated over a particular set of experimental data but are frequently used for the reaction conditions which are far from validation parameters, and this can lead to high uncertainties in the model predictions. The deficit of the experimental data or their high uncertainties do not allow justifying a feasible range of RRCs, model tailoring or final valid parameter range of a kinetic model. In our previous study [17] we introduced the criterion for applicability of an experimental target, E_{ap} (a relation between experimental error and parameter constrain), and showed, that far not all experimental data we have are useful for the RRCs' improvement, also if they have low errors, because these data are not sensitive to the studied RRCs. The measurement planning needs methods for evaluating the problem-oriented operating conditions of experiments. The combination of rigorous methods for uncertainty and consistency analyses of the big amount of data and methods for model optimization is the way to handle kinetic data today. That can be realized only with advanced computing systems like PrIMe [21, 61], which is now in standby modus.

4.2 Laminar flame speeds

The experimental data versus modeling results performed with the studied model and the compared models are presented in Figure 6. The spread of points measured by different groups in Figure 6a shows that uncertainties for laminar flame speeds can be larger than 10% at the peak (φ = 1.1) [60]. As shown in Figure 6, model-1 predicted higher laminar flame speeds than the experimental targets, which was revised by the upgrade work in model-2. The mechanism improvement was achieved by revision RRCs of reactions (R2), (R3), (R4b), and (R5a) (see Table 2 and Supplementary-2). The simulation of laminar flame speeds at various pressures also shows a good agreement with the data measured by Hassan et al. [48]. The compared models, Aramco 3.0 [12], UCSD [13], and USC

2.0 [11], also show acceptable results for the collected data.

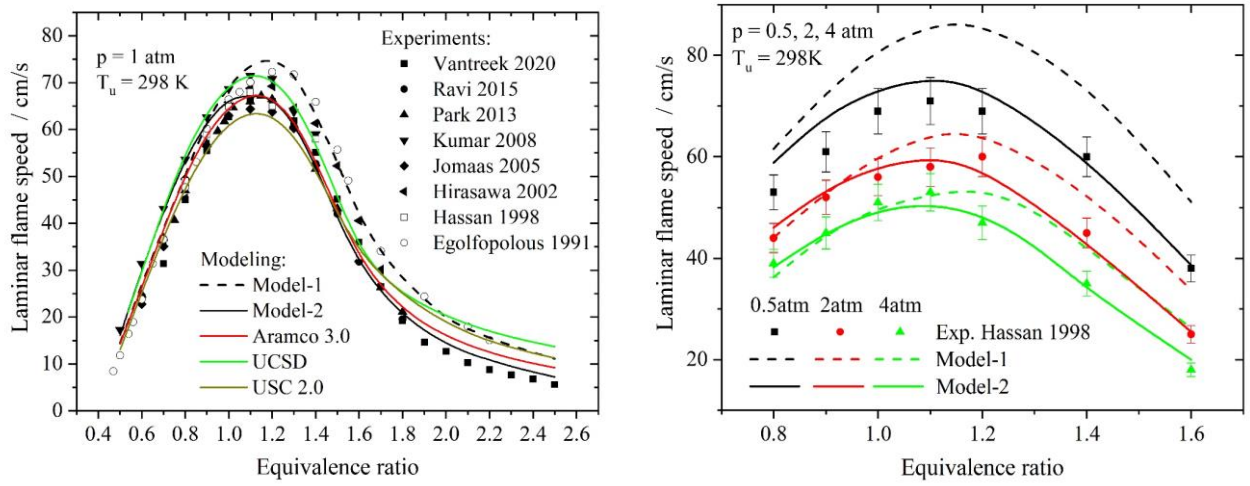

(a) **(b)**

Figure 6. Experimental laminar flame speed data (Hassan et al. [48], Hirasawa et al. [49], Jomaas et al. [50], Ibarreta et al. [8], Kumar et al. [51], Park et al. [52], Ravi et al. [53]) versus modeling results performed with model-1, model-2, Aramco 3.0 [12], UCSD [13], USC 2.0 [11] mechanisms.

4.3 Concentration profiles

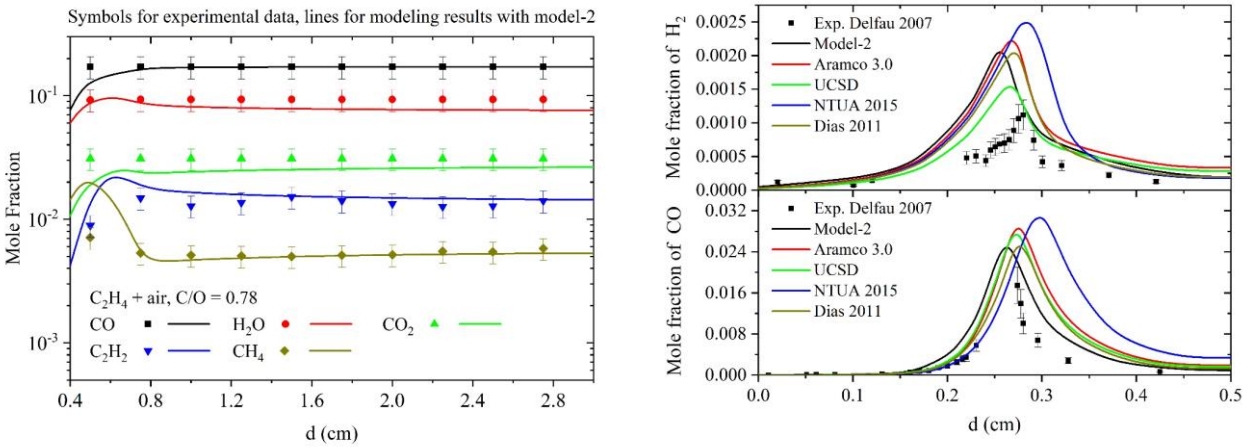

(a) **(b)**

Figure 7. The concentration profiles measured in premixed laminar flame of C_2H_4/air versus modeling results: (a) Xu et al. [55] vs model-2 (b) Delfau et al. [56] vs model-2, Aramco 3.0 mechanism [12], UCSD mechanism [13], USC 2.0 mechanism [11].

Reactions related to C_2H_5, CH_2CO, CH_3CO, and CH_2CHO (reaction R7-14) were triggers of progress in concentration simulations (see Table 2 and Supplementary-2), as they are the key intermediates of C_2H_4 oxidation. Generally, the developed model demonstrates satisfactory agreement with the simulated data. Detailed results are shown in Supplementary-4.

Figure 7 reports simulations of concentration profiles measured in laminar premixed ethylene flames by Xu et al. [55] and Delfau et al. [56]. The last experimental data were recorded in very short flame, above 0.4 cm from the burner. Data of Xu et al. [55] are in excellent accordance with simulations, while data of Delfau et al. [56] are described with some discrepancies, but in accordance with trends and values of simulation results with other models, as shown in Figure 7b.

Compared to the ignition delay time and laminar flame speed data, the concentration profiles demonstrate a higher uncertainty/inconsistency level. Some of the measurement conducted under the similar conditions by different workgroups demonstrate huge discrepancies between reported concentration profiles.

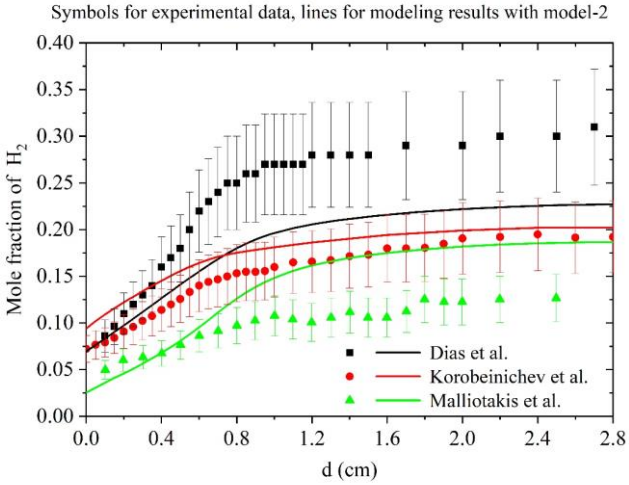

Figure 8. Comparison of H_2 concentration profiles measured by Dias et al. [7], Korobeinichev et al. [57] and Malliotakis et al. [2] (presented with 20% uncertainties) at similar conditions and modeling results simulated with model-2.

Figure 8 presents the concentration profiles of H_2 in fuel rich premixed flat flames measured by Dias et al. [7], Korobeinichev et al. [57] and Malliotakis et al. [2] and the modeling results simulated with the model-2. The three experiments were carried out to investigate the PAH and soot formation in the rich C_2H_4 premixed flames at similar pressure with similar mixing ratio, Table 3. Although the specific settings of the experimental devices are different, all the facilities are designed to obtain ideal one-dimensional premixed flames in flat flame burner. The experimentally determined temperature profiles have been imposed to calculations so that the heat losses to the burner are explicitly taken into

account [2]. Nonetheless, as it can be seen in Figure 8, the difference in results reaches factor of 3. By comparing the data measured by Dias et al. [7] and Malliotakis et al. [2], it can be concluded that difference of 3% in the initial C_2H_4 concentration can lead to a 20% increase in the H_2 mole fraction. To point out which data could be used for the model optimization we performed simulations with the models Aramco 3.0 [12], UCSD [13], Dias et al. [7] and Malliotakis et al. [2] (NTUA 2015) as well. Results of model comparison are shown in Supplementary-4 and will be described in the next section.

Based on these simulations, the RRCs were not fixed for concentration profiles intentionally. The experimentally measured mole fractions are only used for preventing major deviations during the modification work.

4.3 Discussion

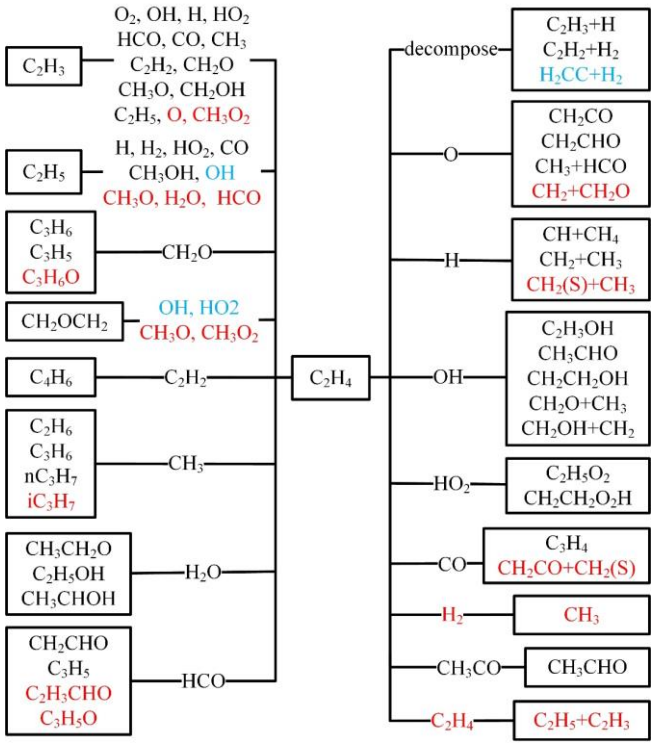

Figure 9. Channels for the initial steps of C_2H_4 oxidation and pyrolysis (coloured in black are the channels which model-1 contains, coloured in red are the channels which model-1 and model-2 lack, coloured in blue are the reactions which have been added to model-2).

Figure 9 summarizes the studied channels for the oxidation of C_2H_4 [2, 6, 7, 11-14, 23] adopted for the model-2 structure. The channels marked with red color were not included in the model due to

their weak impact on the validation data. If these reactions were added in the model, the new RRCs could not be validated by the existing experimental data, so that it is unnecessary to introduce these channels with uncontrollable uncertainties. New channels for C_2H_5, H_2CC and CH_2OCH_2 (blue) were added according to the sensitivity analysis and their important roles in the formation of PAH.

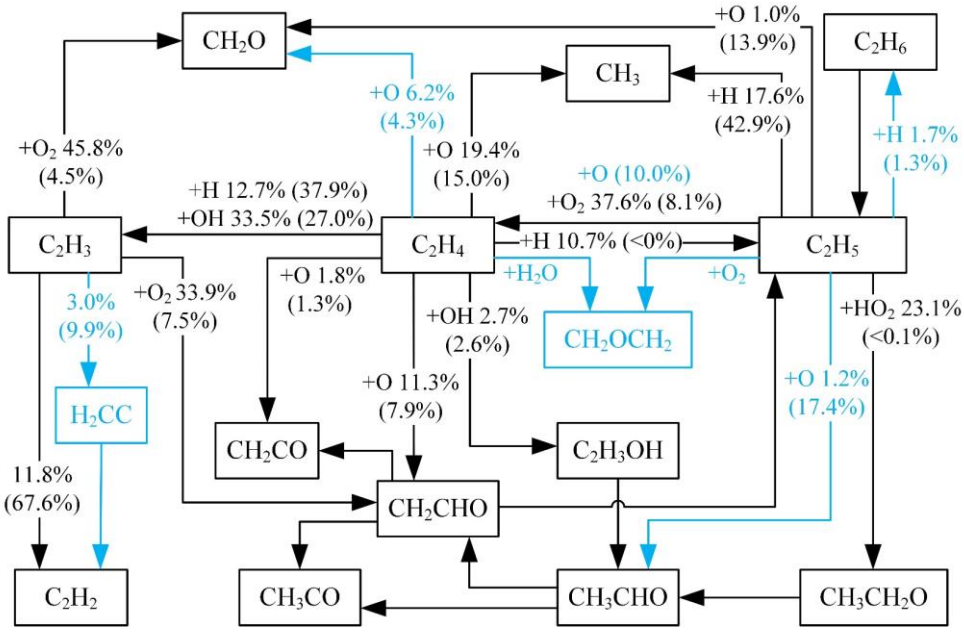

Figure 10. Reaction flow diagrams of C_2H_4 oxidation at φ = 1, p = 1 atm, T = 1000 K (percentages out of the brackets) and T = 1800 K (percentages inside of the brackets) with model-2 (blue colour for the new reactions added in model-2).

Performed improvements of the model-1 resulted in the redistribution of atomic flows simulated with model-2. The percentages for different channels are calculated based on the top 20 rates of productions. Statistical results of rates of production for C_2H_4 oxidation at 1000 K (numbers out of the brackets) and 1800 K (numbers inside the brackets) are shown in Figure 10. New channels added in model-2 are highlighted with color blue. The main changes are related to the reactions of CH_2OCH_2, H_2CC, C_2H_4 and C_2H_5. Channels of CH_2OCH_2, which are important for the low-temperature reactions, are added as new paths. Reactions of C_2H_4+O and C_2H_5+O are revised and found to play an important role in the high-temperature condition. The RRCs of C_2H_4+O channels are replaced by the newest recommendations of Morin et al. [62, 63]. The channels from C_2H_4 to PAH precursors (C_2H_2, H_2CC,

C_2H_3) are rebuilt following the work of Laskin et al. [64] and Wang et al. [65]. The detailed update work and discussion on the RRCs are shown in Supplementary-2.

Table 4. Validation information and average errors for ignition delay times and laminar flame speeds for C_2H_4 and C_2H_2 with model-1 and model-2.

Mechanism	Average error E for C_2H_4 ignition delay times	Average error E for C_2H_2 ignition delay times	Average error E for C_2H_4 laminar flame speeds
Model-2	0.00163	0.00092	4.35
Model-1	0.00394	0.00098	7.32

The final list of new reactions and sources of their RRCs is given in Table S2-2 in Supplementary-2. The final obtained capabilities in comparison to model-1 are integrated in Table 4. Significant improvement is made to the C_2H_4 oxidation model by the upgrade work and the prediction ability for C_2H_2 oxidation [17, 66-69] is retained as well.

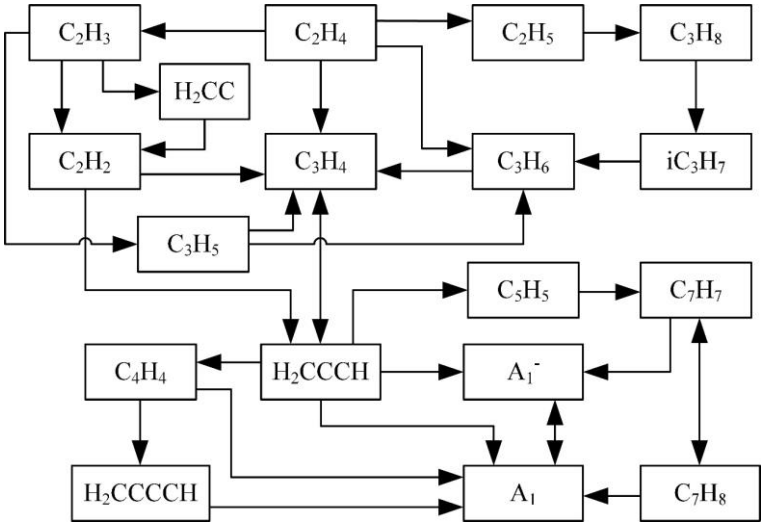

Figure 11. Reaction flow diagram of C_2H_4 to benzene (A_1) in the simulation of premixed laminar flame of Korobeinichev et al. [57] with model-2.

The reaction flow diagram from C_2H_4 to benzene (A_1) of model-2, presented in Figure 11, fixes the actual logic of aromatic molecule formation and main directions of the following work: reactions of C_2H_6, C_2H_5 and C_2H_5OH will be further investigated followed by sub-mechanisms of C_3H_4, C_3H_6, and C_3H_8.

4.5 Comparison of mechanisms

In the following paragraph, we would like to briefly present a comparison of reaction models once

again to focus on the problem of the structure of a chemical reaction model and its valid parameter range. As the different criteria for defining the valid model parameter range are based on the sensitivity coefficients [70], we highlight the problem using the results of sensitivity analysis of ignition delay times to RRCs performed for four models: model-2 (115 species, 971 reactions), Aramco 3.0 [12] (581 species, 3037 reactions), USC 2.0 [11] (111 species, 784 reactions) and UCSD [13] (58 species 207 reactions) at T_5 = 1000 K and 1800 K, Figure 12. Detailed comparison of measured ignition delay times and modeling results with model-1, model-2, Aramco 3.0 [12] and UCSD [13] are shown in Supplementary-3.

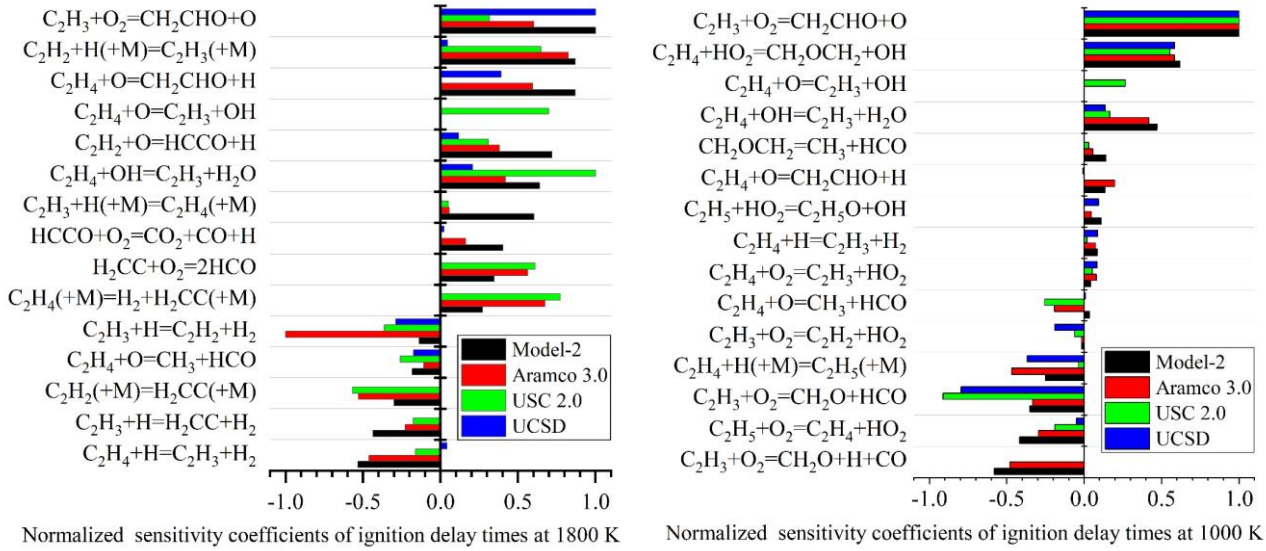

Figure 12. Comparison of normalized sensitivity coefficients of ignition delay times simulated with model-2 (this study), Aramco 3.0 [12], USC 2.0 [11] and UCSD [13] to the RRCs for C_2H_4/O_2/Ar mixture with φ = 1.0, p_5 = 1 atm and (a) T_5 = 1000 K; (b) T_5 = 1800 K.

For the condition of T_5 = 1000 K, the most obvious discrepancies among these models occur in the channels of $C_2H_3+O_2=CH_2O+H+CO$, $C_2H_3+O_2=CH_2O+HCO$, and $C_2H_3+O_2=C_2H_2+HO_2$. The model-2 and Aramco 3.0, which have the RRCs for reactions of $C_2H_3+O_2$ adopted from Goldsmith et al. [71], show the similar sensitivities to these channels compared to the other two models, which have RRCs from [72, 73]. For all the models, channel $C_2H_3+O_2=CH_2CHO+O$ demonstrates the highest importance at lower temperature, Figure 12a.

For higher temperatures, the distribution between sensitivity coefficients obtained for analyzed models is much higher and for the reaction $C_2H_4+H=C_2H_3+H_2$ they are even opposite: in the model UCSD [13], this reaction has a negative effect on the ignition delay times, Figure 12b. The UCSD model lacks the component H_2CC, which is the important product of C_2H_4 decomposition at high temperature, as shown in Figure 12b. The highest sensitivity of the ignition delay time to reaction $C_2H_3+H=C_2H_2+H_2$ demonstrated by the model of Aramco 3.0 [12] can be explained with the modification performed in this mechanism: the RRC of this channel has been increased to a much higher value than the recommendations [31, 33]. Reaction $C_2H_4+O=C_2H_3+OH$ of the USC 2.0 model shows the importance for both low- and high-temperature conditions, but this channel tends to be an overall reaction and was not studied in the newest works [63, 74-76].

Apparent disagreements in the sensitivity coefficients follow from various distributions of atom fluxes in the models, which in turn are defined with individual combinations between the reaction channels and correlations between the rate parameters. Differences in the model structures can be unnoticeable at the simulation of macro processes: analyzed reaction mechanisms are different in choices of elementary reactions and their rate parameters, but the ignition delay times are reproduced well with all analyzed models in most cases (detailed comparisons of measured ignition delay times and modeling results are shown in Supplementary-3).

Average errors (equation 6) for C_2H_4 ignition delay times simulated with model-1, model-2, and mechanisms [6, 11-14, 17, 23, 73] are listed in Table 5. As expected, the updated new mechanism with its specific adaptation for C_2H_4 yields generally better results in comparison with the analyzed models. The highest errors among the compared mechanisms were obtained for models of Dias et al. [7] and NTUA [2] following from the process of model construction. These two reaction mechanisms were developed based on measurements performed by authors of [2, 7] in premixed laminar flame. The application scope of these models [2, 7] might be restricted without comprehensive research. The high error value shown by GRI 3.0 [23] logically follows from the limitation of available experimental data

during the creation of the model.

Table 5. Validation information and average errors for C_2H_4 ignition delay times simulated by different mechanisms.

Mechanism	Year	Recent validation for C_2H_4	Average error for C_2H_4	Average error for C_2H_2
Model-2 (this study)	2021	this study	0.00163	0.00092
Aramco 3.0 [12]	2018	Kopp et al. 2014 [77]	0.00183	0.00085
UCSD [13]	2016	UCSD 2015 [13]	0.00380	0.00089
Lopez et al. [6]	2009	Lopez et al. 2009 [6]	0.00386	0.00397
Model-1 [17]	2019	None	0.00394	0.00098
USC 2.0 [11]	2009	None	0.00497	0.00236
Konnov [14]	2009	None	0.00508	0.00305
GRI 3.0 [23]	1999	None	0.01856	0.01019
Dias et al. [7]	2011	Dias et al. 2011 [7]	0.01890	0.00550
NTUA 2015 [2]	2015	Malliotakis et al [2]	0.03635	0.00453

It can be concluded from the figured dominance channels for modeled processes, Figure 12, are mostly related to the individual model structure and not to the nature of the process. In any case we do not have criteria to recognize that and simple enumerating the chemical species and elementary reactions with used RRCs are not enough for that. The special objective methods should be developed for evaluating the model structure quality and tools for model comparison. It is worth mentioning that simple adaptations of RRCs from different mechanisms may jeopardize the prediction capabilities of mechanism by implementing a weighting factor for this reaction which does not fit.

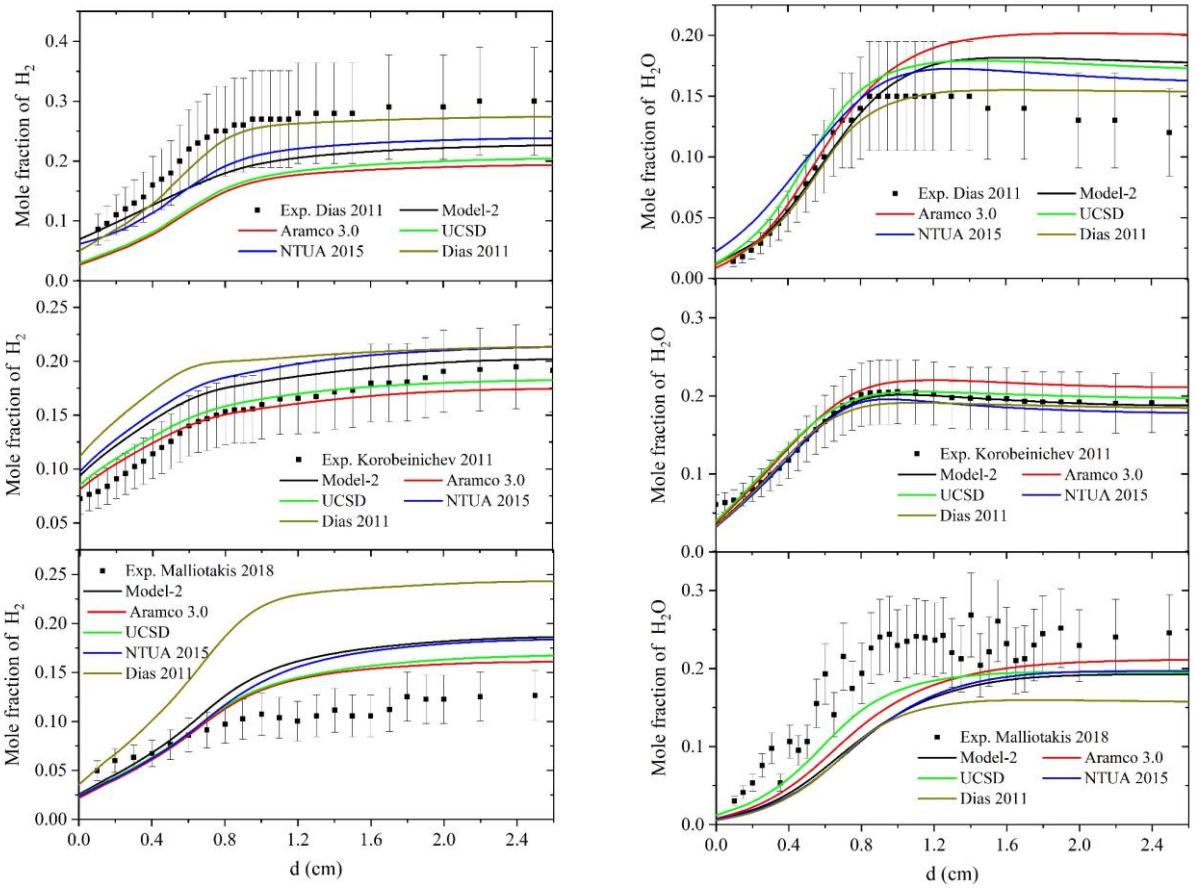

(a) **(b)**

Figure 13. Comparison of the concentration profiles measured by Dias et al. [7], Korobeinichev et al. [57] and Malliotakis et al. [2] and simulation results obtained with model-2, Aramco 3.0 [12], UCSD [13], Dias 2011 [7] and NTUA 2015 (Malliotakis et al.) [2]: (a) mole fractions of H_2; (b) mole fractions of H_2O.

Modeling concentration profiles especially clearly demonstrates the effect of model structure on the results. Unfortunately, the lack of such data and some inconsistencies of the available data do not allow us to draw final conclusions and use these data for final model optimization.

The calculations of the concentration profiles of H_2 and H_2O with five models (model-2 and Aramco 3.0 [12], UCSD [13], Dias 2011 [7] and NTUA [2]) are compared with the measured data obtained in [7], [57] and [2], as shown in Figure 13. As it was previously described, these data obtained under similar conditions, Table 3, are not consistent, Figure 8. Data of Korobeinichev et al. [57] are predicted within their experimental errors by all models, excepting models of Dias et al. [7] and NTUA

[2] developed for the restricted calibration conditions and having the highest error for most of the concentration profiles. No model describes hydrogen profile measured by Malliotakis et al. [2]; all models have a trend to under-predict results of Dias et al. [7] and to over-predict results of Malliotakis et al. [2] for H_2. The opposite results are obtained for H_2O simulations: all studied models over-predict the experimental data from Dias et al. [7] und under-predict the data of Malliotakis et al. [2]. The Aramco 3.0 [12] mechanism shows the lowest values for hydrogen concentration and the highest values for water concentration measured in [7], [57] and [2] data, as shown in Figure 13.

6. Conclusion

The upgrade and extension of the detailed C_2H_4 combustion mechanism have been successfully performed based on the simulations of the experimental data for auto-ignition [1, 3, 5, 43-47], premixed laminar flame speeds [48-54, 58], and concentration profiles measured in premixed flat flame [2, 7, 55-57]. Hundreds of heterogenic experimental targets measured over a wide spectrum of experimental conditions by different research groups have been analyzed for model optimization. Sensitivity and rate of production analyses have been conducted to identify the key reactions and intermediates. The selected modifications of RRCs were performed within the uncertainty intervals estimated with statistical methods. The following features have been studied:

(1) Initial reaction paths of the C_2H_4 oxidation and pyrolysis, including channels related to the newly added H_2CC, CH_2OCH_2, and CH_2OCH (reaction R15-26);

(2) Pressure-dependent reaction rate coefficients for reactions of C_2H_4+OH, C_2H_5+O_2, CH_2CO, CH_3CO, and CH_2CHO (reaction R3, R7, and R11-14);

(3) Reactions of C_2H_4+HO_2, CH_2OCH_2, and CH_2OCH (reaction R6, R7a, and R21-26) for the low-temperature chemistry;

(4) Reactions related to the key intermediates for the aromatic precursor formation (C_2H_2, H_2CC, C_2H_3, and C_2H_5).

Comparison with the other chemical kinetic models [2, 6, 7, 11-14, 23] shows that the updated model demonstrates a good ability to predict auto-ignition delay times and laminar flame speeds, and satisfactory results for reproduction of concentration profiles. The model is well prepared for the next step of optimization: upgrade of C_2H_6 and C_2H_5OH sub-mechanisms and further improvement of the PAH formations reaction paths [2, 7, 57].

Problems of the inconsistency of the experimental data have been shown and discussed. The reported conflicting results of the used experimental data, measured by the different groups make it difficult to draw the final univocal conclusions about the studied kinetic model optimization.

More effort should be put into the development of the methods and numerical tools for the model quality analysis, data uncertainty, uncertainty propagation analyses and evaluation of the model valid parameter range. The simple comparison of simulations with measured data cannot be considered as a final assessment of model quality and model ability to reproduce the real natural micro-processes. Without such objective assessments, the different reaction mechanisms can be regarded as statistical samplings for gathering information about process and to make some assumptions about the entire system's behaviour.

6. Acknowledgments

The authors would like to thank China Scholarship Council, and acknowledge the Ministry of Education and Science of Republic of Kazakhstan for funding this work through the project IRN AP05133755. The authors would also like to acknowledge the full financial support of one of the co-authors, Mrs. Kanz, by the DAAD German Academic Exchange Service within the framework of DLR-DAAD Research Fellowship.

References

[1] J. Shao, D.F. Davidson, R.K. Hanson, A shock tube study of ignition delay times in diluted methane, ethylene, propene and their blends at elevated pressures, Fuel 225 (2018) 370-380.

[2] Z. Malliotakis, N. Leplat, G. Vourliotakis, C. Keramiotis, G. Skevis, M.A. Founti, J. Vandooren, An Experimental and Detailed Chemical Kinetic Investigation of the Addition of C2 Oxygenated Species in Rich Ethylene Premixed Flames, Combustion Science and Technology, (2018) 1-24.
[3] M.M. Kopp, N.S. Donato, E.L. Petersen, W.K. Metcalfe, S.M. Burke, H.J. Curran, Oxidation of Ethylene–Air Mixtures at Elevated Pressures, Part 1: Experimental Results, Journal of Propulsion and Power 30 (2014) 790-798.
[4] C. Xu, A.A. Konnov, Validation and analysis of detailed kinetic models for ethylene combustion, Energy 43 (2012) 19-29.
[5] S. Saxena, M.S.P. Kahandawala, S.S. Sidhu, A shock tube study of ignition delay in the combustion of ethylene, Combustion and Flame 158 (2011) 1019-1031.
[6] J.G. Lopez, C.L. Rasmussen, M.U. Alzueta, Y. Gao, P. Marshall, P. Glarborg, Experimental and kinetic modeling study of C2H4 oxidation at high pressure, Proceedings of the Combustion Institute 32 (2009) 367-375.
[7] V. Dias, J. Vandooren, Experimental and modeling studies of C2H4/O2/Ar, C2H4/methylal/O2/Ar and C2H4/ethylal/O2/Ar rich flames and the effect of oxygenated additives, Combustion and Flame 158 (2011) 848-859.
[8] A.F. Ibarreta, C.-J. Sung, H. Wang, Experimental characterization of premixed spherical ethylene/air flames under sooting conditions, Proceedings of the Combustion Institute 31 (2007) 1047-1054.
[9] V. Chernov, M.J. Thomson, S.B. Dworkin, N.A. Slavinskaya, U. Riedel, Soot formation with C1 and C2 fuels using an improved chemical mechanism for PAH growth, Combustion and Flame 161 (2014) 592-601.
[10] S.B. Dworkin, Q. Zhang, M.J. Thomson, N.A. Slavinskaya, U. Riedel, Application of an enhanced PAH growth model to soot formation in a laminar coflow ethylene/air diffusion flame, Combustion and Flame 158 (2011) 1682-1695.
[11] H. Wang, X. You, A.V. Joshi, S.G. Davis, A. Laskin, F. Egolfopoulos, C.K. Law, USC Mech Version II. High-Temperature Combustion Reaction Model of H2/CO/C1-C4 Compounds., http://ignis.usc.edu/USC_Mech_II.htm, (May 2007).
[12] C.-W. Zhou, Y. Li, U. Burke, C. Banyon, K.P. Somers, S. Ding, S. Khan, J.W. Hargis, T. Sikes, O. Mathieu, E.L. Petersen, M. AlAbbad, A. Farooq, Y. Pan, Y. Zhang, Z. Huang, J. Lopez, Z. Loparo, S.S. Vasu, H.J. Curran, An experimental and chemical kinetic modeling study of 1,3-butadiene combustion: Ignition delay time and laminar flame speed measurements, Combustion and Flame 197 (2018) 423-438.

[13] Chemical-Kinetic Mechanisms for Combustion Applications, Mechanical and Aerospace Engineering (Combustion Research), University of California at San Diego, San Diego Mechanism web page, http://combustion.ucsd.edu.

[14] A.A. Konnov, Implementation of the NCN pathway of prompt-NO formation in the detailed reaction mechanism, Combustion and Flame 156 (2009) 2093-2105.

[15] Z. Qin, V.V. Lissianski, H. Yang, W.C. Gardiner, S.G. Davis, H. Wang, Combustion chemistry of propane: a case study of detailed reaction mechanism optimization, Proceedings of the Combustion Institute 28 (2000) 1663-1669.

[16] G. Eckel, J. Grohmann, L. Cantu, N. Slavinskaya, T. Kathrotia, M. Rachner, P. Le Clercq, W. Meier, M. Aigner, LES of a swirl-stabilized kerosene spray flame with a multi-component vaporization model and detailed chemistry, Combustion and Flame 207 (2019) 134-152.

[17] N. Slavinskaya, A. Mirzayeva, R. Whitside, J. Starke, M. Abbasi, M. Auyelkhankyzy, V. Chernov, A modelling study of acetylene oxidation and pyrolysis, Combustion and flame 210 (2019) 25-42.

[18] N.A. Slavinskaya, U. Riedel, S.B. Dworkin, M.J. Thomson, Detailed numerical modeling of PAH formation and growth in non-premixed ethylene and ethane flames, Combustion and Flame 159 (2012) 979-995.

[19] A.M. Valencia-López, F. Bustamante, A. Loukou, B. Stelzner, D. Trimis, M. Frenklach, N.A. Slavinskaya, Effect of benzene doping on soot precursors formation in non-premixed flames of producer gas (PG), Combustion and Flame 207 (2019) 265-280.

[20] N. Slavinskaya, M. Abbasi, J.-H. Starcke, A. Mirzayeva, O.J. Haidn. Skeletal mechanism of the methane oxidation for space propulsion applications. In: editor^editors. 52nd AIAA/SAE/ASEE Joint Propulsion Conference; 2016. p. 4781.

[21] N. Slavinskaya, M. Abbasi, J.H. Starcke, R. Whitside, A. Mirzayeva, U. Riedel, W. Li, J. Oreluk, A. Hegde, A. Packard, Development of an uncertainty quantification predictive chemical reaction model for syngas combustion, Energy & Fuels 31 (2017) 2274-2297.

[22] M.E. DESIGNS, Chemkin-pro, (2011).

[23] G.P. Smith, D.M. Golden, M. Frenklach, N.W. Moriarty, B. Eiteneer, M. Goldenberg, C.T. Bowman, R.K. Hanson, S. Song, W.C. Gardiner Jr, GRI 3.0 Mechanism, Gas Research Institute (http://www.me.berkeley.edu/gri_mech), (1999).

[24] L.R. Fokin, N. Slavinskaya, Thermophysical parameter correlation for low-density gas mixtures: Ar-Xe, Institute for High Temperatures, USSR Academy of Sciences 25 (1987) 40-45.

[25] S. Sokolov, I. Silin, "Preprint JINR D-810," Dubna, (1961).

[26] V. Kurbatov, I. Silin, New method for minimizing regular functions with constraints on parameter region, Nuclear Instruments and Methods in Physics Research Section A 345 (1994) 346-350.
[27] D.L. Baulch, C.T. Bowman, C.J. Cobos, R.A. Cox, T. Just, J.A. Kerr, M.J. Pilling, D. Stocker, J. Troe, W. Tsang, R.W. Walker, J. Warnatz, Evaluated Kinetic Data for Combustion Modeling: Supplement II, Journal of Physical and Chemical Reference Data 34 (2005) 757-1397.
[28] T. Nagy, É. Valkó, I. Sedyó, I.G. Zsély, M.J. Pilling, T. Turányi, Uncertainty of the rate parameters of several important elementary reactions of the H2 and syngas combustion systems, Combustion and Flame 162 (2015) 2059-2076.
[29] J. Manion, R. Huie, R. Levin, D. Burgess Jr, V. Orkin, W. Tsang, W. McGivern, J. Hudgens, V. Knyazev, D. Atkinson, NIST chemical kinetics database, NIST standard reference database 17 (2008) 20899-28320.
[30] D. Baulch, M. Bowers, D. Malcolm, R. Tuckerman, Evaluated Kinetic Data for High-Temperature Reactions. Volume 5. Part 1. Homogeneous Gas Phase Reactions of the Hydroxyl Radical with Alkanes, Journal of physical and chemical reference data 15 (1986) 465-592.
[31] D. Baulch, C. Cobos, R. Cox, C. Esser, P. Frank, Th. Just, JA Kerr, MJ Pilling, J. Troe, RW Walker, and J. Warnatz, Journal of Physical and Chemical Reference Data 21 (1992) 411-569.
[32] D.L. Baulch, C.J. Cobos, R.A. Cox, P. Frank, G. Hayman, T. Just, J.A. Kerr, T. Murrells, M.J. Pilling, J. Troe, R.W. Walker, J. Warnatz, Evaluated Kinetic Data for Combustion Modeling. Supplement I, Journal of Physical and Chemical Reference Data 23 (1994) 847-848.
[33] J. Warnatz, Rate coefficients in the C/H/O system, Combustion chemistry, Springer1984, pp. 197-360.
[34] W. Tsang, R.F. Hampson, Chemical Kinetic Data Base for Combustion Chemistry. Part I. Methane and Related Compounds, Journal of Physical and Chemical Reference Data 15 (1986) 1087-1279.
[35] M.A. Ali, B. Upendra, B. Rajakumar, Kinetic parameters of abstraction reactions of OH radical with ethylene, fluoroethylene, cis-and trans-1, 2-difluoroethylene and 1, 1-difluoroethylene, in the temperature range of 200–400 K: Gaussian-3/B3LYP theory, Chemical Physics Letters 511 (2011) 440-446.
[36] J.P. Senosiain, S.J. Klippenstein, J.A. Miller, Reaction of ethylene with hydroxyl radicals: a theoretical study, The Journal of Physical Chemistry A 110 (2006) 6960-6970.
[37] G. Liu, Y. Ding, Z. Li, Q. Fu, X. Huang, C. Sun, A. Tang, Theoretical study on mechanisms of the high-temperature reactions C2H3 + H2O and C2H4 + OH, Physical Chemistry Chemical Physics 4 (2002) 1021-1027.

[38] C.K. Westbrook, M.M. Thornton, W.J. Pitz, P.C. Malte, A kinetic study of ethylene oxidation in a well-stirred reactor, Symposium (International) on Combustion 22 (1989) 863-871.
[39] F.P. Tully, Hydrogen-atom abstraction from alkenes by OH, ethene and 1-butene, Chemical Physics Letters 143 (1988) 510-514.
[40] A.-D. Liu, W.A. Mulac, C.D. Jonah, Pulse radiolysis study of the reaction of OH radicals with C2H4 over the temperature range 343-1173 K, International Journal of Chemical Kinetics 19 (1987) 25-34.
[41] K. Hughes, T. Turányi, A. Clague, M. Pilling, Development and testing of a comprehensive chemical mechanism for the oxidation of methane, International Journal of Chemical Kinetics 33 (2001) 513-538.
[42] N. Slavinskaya, P. Frank, A modelling study of aromatic soot precursors formation in laminar methane and ethene flames, Combustion and Flame 156 (2009) 1705-1722.
[43] C.J. Brown, G.O. Thomas, Experimental studies of shock-induced ignition and transition to detonation in ethylene and propane mixtures, Combustion and Flame 117 (1999) 861-870.
[44] M.B. Colket, L.J. Spadaccini, Scramjet Fuels Autoignition Study, Journal of Propulsion and Power 17 (2001) 315-323.
[45] D.M. Kalitan, J.M. Hall, E.L. Petersen, Ignition and Oxidation of Ethylene-Oxygen-Diluent Mixtures with and Without Silane, Journal of Propulsion and Power 21 (2005) 1045-1056.
[46] O.G. Penyazkov, K.L. Sevrouk, V. Tangirala, N. Joshi, High-pressure ethylene oxidation behind reflected shock waves, Proceedings of the Combustion Institute 32 (2009) 2421-2428.
[47] F. Deng, Y. Pan, W. Sun, F. Yang, Y. Zhang, Z. Huang, Comparative Study of the Effects of Nitrous Oxide and Oxygen on Ethylene Ignition, Energy & Fuels 31 (2017) 14116-14128.
[48] M.I. Hassan, K.T. Aung, O.C. Kwon, G.M. Faeth, Properties of Laminar Premixed Hydrocarbon/Air Flames at Various Pressures, Journal of Propulsion and Power 14 (1998) 479-488.
[49] T. Hirasawa, C.J. Sung, A. Joshi, Z. Yang, H. Wang, C.K. Law, Determination of laminar flame speeds using digital particle image velocimetry: Binary Fuel blends of ethylene, n-Butane, and toluene, Proceedings of the Combustion Institute 29 (2002) 1427-1434.
[50] G. Jomaas, X.L. Zheng, D.L. Zhu, C.K. Law, Experimental determination of counterflow ignition temperatures and laminar flame speeds of C2–C3 hydrocarbons at atmospheric and elevated pressures, Proceedings of the Combustion Institute 30 (2005) 193-200.
[51] K. Kumar, G. Mittal, C. Sung, C. Law, An experimental investigation of ethylene/O2/diluent mixtures: Laminar flame speeds with preheat and ignition delays at high pressures, Combustion and Flame 153 (2008) 343-354.

[52] O. Park, P.S. Veloo, F.N. Egolfopoulos, Flame studies of C2 hydrocarbons, Proceedings of the Combustion Institute 34 (2013) 711-718.
[53] S. Ravi, T.G. Sikes, A. Morones, C.L. Keesee, E.L. Petersen, Comparative study on the laminar flame speed enhancement of methane with ethane and ethylene addition, Proceedings of the Combustion Institute 35 (2015) 679-686.
[54] L. Van Treek, N. Roth, L. Seidel, F. Mauß, Measurements of the laminar burning velocities of rich ethylene/air mixtures, Fuel 275 (2020) 117938.
[55] F. Xu, P. Sunderland, G. Faeth, Soot formation in laminar premixed ethylene/air flames at atmospheric pressure, Combustion and Flame 108 (1997) 471-493.
[56] J.-L. Delfau, J. Biet, M. Idir, L. Pillier, C. Vovelle, Experimental and numerical study of premixed, lean ethylene flames, Proceedings of the Combustion Institute 31 (2007) 357-365.
[57] O.P. Korobeinichev, S.A. Yakimov, D.A. Knyazkov, T.A. Bolshova, A.G. Shmakov, J. Yang, F. Qi, A study of low-pressure premixed ethylene flame with and without ethanol using photoionization mass spectrometry and modeling, Proceedings of the Combustion Institute 33 (2011) 569-576.
[58] F.N. Egolfopoulos, D.L. Zhu, C.K. Law, Experimental and numerical determination of laminar flame speeds: Mixtures of C2-hydrocarbons with oxygen and nitrogen, Symposium (International) on Combustion 23 (1991) 471-478.
[59] C. Olm, T. Varga, É. Valkó, S. Hartl, C. Hasse, T. Turányi, Development of an Ethanol Combustion Mechanism Based on a Hierarchical Optimization Approach, International Journal of Chemical Kinetics 48 (2016) 423-441.
[60] G. Walter, H. Wang, A. Kanz, A. Kolbasseff, X. Xu, O. Haidn, N. Slavinskaya, Experimental error assessment of laminar flame speed measurements for digital chemical kinetics databases, Fuel 266 (2020).
[61] X. You, A. Packard, M. Frenklach, Process informatics tools for predictive modeling: Hydrogen combustion, International Journal of Chemical Kinetics 44 (2012) 101-116.
[62] J. Morin, Y. Bedjanian, Reaction of O (3P) with C2H4: Yield of the Reaction Products as a Function of Temperature, The Journal of Physical Chemistry A 120 (2016) 9063-9070.
[63] J. Morin, Y. Bedjanian, M.N. Romanias, Rate Constants of the Reactions of O (3P) Atoms with Ethene and Propene over the Temperature Range 230–900 K, International Journal of Chemical Kinetics 49 (2017) 53-60.
[64] A. Laskin, H. Wang, C.K. Law, Detailed kinetic modeling of 1,3-butadiene oxidation at high temperatures, International Journal of Chemical Kinetics 32 (2000) 589-614.

[65] H. Wang, A new mechanism for initiation of free-radical chain reactions during high-temperature, homogeneous oxidation of unsaturated hydrocarbons: Ethylene, propyne, and allene, International Journal of Chemical Kinetics 33 (2001) 698-706.
[66] M. Rickard, J. Hall, E. Petersen, Effect of silane addition on acetylene ignition behind reflected shock waves, Proceedings of the Combustion Institute 30 (2005) 1915-1923.
[67] B. Eiteneer, M. Frenklach, Experimental and modeling study of shock-tube oxidation of acetylene, International Journal of Chemical Kinetics 35 (2003) 391-414.
[68] Y. Hidaka, K. Hattori, T. Okuno, K. Inami, T. Abe, T. Koike, Shock-tube and modeling study of acetylene pyrolysis and oxidation, Combustion and Flame 107 (1996) 401-417.
[69] R. Fournet, J. Bauge, F. Battin-Leclerc, Experimental and modeling of oxidation of acetylene, propyne, allene and 1, 3-butadiene, International journal of chemical kinetics 31 (1999) 361-379.
[70] H. Wang, D.A. Sheen, Combustion kinetic model uncertainty quantification, propagation and minimization, Progress in Energy and Combustion Science 47 (2015) 1-31.
[71] C.F. Goldsmith, L.B. Harding, Y. Georgievskii, J.A. Miller, S.J. Klippenstein, Temperature and pressure-dependent rate coefficients for the reaction of vinyl radical with molecular oxygen, The Journal of Physical Chemistry A 119 (2015) 7766-7779.
[72] A. Mebel, E. Diau, M. Lin, K. Morokuma, Ab initio and RRKM calculations for multichannel rate constants of the C2H3+ O2 reaction, Journal of the American Chemical Society 118 (1996) 9759-9771.
[73] N.M. Marinov, W.J. Pitz, C.K. Westbrook, A.M. Vincitore, M.J. Castaldi, S.M. Senkan, C.F. Melius, Aromatic and Polycyclic Aromatic Hydrocarbon Formation in a Laminar Premixed n-Butane Flame, Combustion and Flame 114 (1998) 192-213.
[74] T.L. Nguyen, L. Vereecken, X.J. Hou, M.T. Nguyen, J. Peeters, Potential energy surfaces, product distributions and thermal rate coefficients of the reaction of O(3P) with C2H4(X1Ag): a comprehensive theoretical study, The Journal of Physical Chemistry A 109 (2005) 7489-7499.
[75] N. Balucani, F. Leonori, P. Casavecchia, B. Fu, J.M. Bowman, Crossed molecular beams and quasiclassical trajectory surface hopping studies of the multichannel nonadiabatic O (3P)+ ethylene reaction at high collision energy, The Journal of Physical Chemistry A 119 (2015) 12498-12511.
[76] X. Li, A.W. Jasper, J. Zádor, J.A. Miller, S.J. Klippenstein, Theoretical kinetics of O + C2H4, Proceedings of the Combustion Institute 36 (2017) 219-227.
[77] M.M. Kopp, E.L. Petersen, W.K. Metcalfe, S.M. Burke, H.J. Curran, Oxidation of Ethylene—Air Mixtures at Elevated Pressures, Part 2: Chemical Kinetics, Journal of Propulsion and Power 30 (2014) 799-811.